

## The New analytical Solution of Unsteady Squeezing Flow under effect No Slip and Slip by using Perturbation Iteration Technique

Hassan R. Shool<sup>1</sup>, Ahmed K. Al-Jaberi<sup>2</sup>, and Abeer Majeed Jasim<sup>3</sup>

<sup>1,2</sup> Department of Mathematics, College of Education for Pure Science, University of Basrah, <sup>3</sup> Department of Mathematics, College of Science, University of Basrah, Basrah, Iraq.

Corresponding Author: [ahmed.shanan@uobasrah.edu.iq](mailto:ahmed.shanan@uobasrah.edu.iq)

### Abstract

The present article analyzes a viscous magneto-hydrodynamic (MHD) of two-dimensional unsteady squeezing fluid flow passing in porous medium between two infinite parallel plates under the effect of no slip and slip at the boundaries. The appropriate similarity transformations are used to obtain a nonlinear ordinary differential equation containing Reynolds number ( $R_E$ ), magneto-hydrodynamic parameter ( $M_G$ ), porous parameter ( $M_P$ ) and slip parameter ( $\vartheta$ ) as physical parameters. The phenomena of the fluid are studied through the investigation of the normal velocity and longitudinal velocity when the two plates are seen to approach each other symmetrically, this causes squeezing to flow. The velocity distributions of modeling problem are obtained for different values of both parameters by using perturbation iteration technique (PIT). Furthermore, the influence of the flow parameters is discussed with the help of graphs. Comparing new approximate solutions of PIT with the Homotopy Perturbation Method (HPM), numerically by using Runge-Kutta Fehlberg (RKF5) and Runge-Kutta of fourth order (RK4) proved the excellent agreement of the proposed technique. Convergence analysis and error estimation is given to foresee the accuracy of approximate analytical solutions.

**Keyword.** Magneto-hydrodynamic, squeezing flow, slip and no slip boundaries, physical parameters, perturbation iteration technique.

### 1. Introduction

The phenomenon of squeezing flow can be seen in many machines' tools and hydrodynamical.

Especially the subject of fluid squeezing between two parallel parts. So many applications that

one might notice these flows in chemical industries, engineering and the food [1-4]. Some examples like pressing, injection, modeling of lubrication and polymer Handling. In the 19th century, flow pressure modeling started and from then onwards, in various fields many interests due to its endless applications. Preliminary studies of these flow are

carried out by Stefan [5], applied to the Newtonian fluid and found an asymptote solution. Consequently, the study of liquids in the electromagnetic field is exceptional an interesting field of magnetic-hydrodynamics

(MHD). The use of magnetic-hydrodynamics fluid as a lubricant is interesting, since under certain extreme circumstances, it avoids the unexpected Lubricant viscosity changes with temperature. Make et al. [6] studied the magnetic-hydrodynamics field such lubricant externally pressurized thrust bearing. Various authors have studied effect of magnetic field on fluid flow. The flow squeezing between two disks with presence of a magnetic field has been examined in [7], and that between rotary disks have been investigated in [8,9]. Porous medium is material that has fluid filled pores, which possesses the characteristics are:

- Permeability: It is the fluid that passes through the porosity and porous medium.
- Porosity: It is characterized as the sum of liquids retained by the fabric.

The porous medium has many applications in this field of reservoir, chemical engineering and petroleum [10]. As the study of slip in a porous medium is difficult to calculate or observe directly [11]. Therefore, most of the studies and observations depend on numerical methods and theoretical analysis, the affirmation of slip approved experimentally through indirect schemes [12]. Considering slip results in increasing computational time and error, and for this reason theoretical analyses are ignored [13, 14]. The impact of slip is an established boundary condition, at a fluid-solid interface, and it has various scientific and technological applications, for example, fluid transportation, rheometric measurements, material processing [15]. The boundary condition of a viscous fluid can be described at the macroscopic level as no-slip [13], this means that the instantaneous velocity will be vanish at the boundary. However, any momentary slip conditions due to shear stress are also verified by the effects of a sudden decrease in viscosity or an arising in flow rates. In fluid mechanics this slip condition is called as the apparent slip. Mooney [16] implemented pioneering work on the subject of slip analysis and was able to define the explicit formulas for slip and fluidity. Slip state handling techniques are important for fluid flow investigation. Moreover, it is generally ignored or underestimated in investigations including complex fluid systems [17,18]. In this study, an unsteady squeezing flow with slip and no-slip conditions at the boundary analyzed and solved by using perturbation iteration technique PIT [19,20]. The results of PIT were compared with HPM and numerically by using RKF5. The planning of this study is as follows: Section 2 introduces the derivation of the proposed problem. Section 3 shows the basic idea of perturbation iteration technique for solving the magneto-hydrodynamics squeezing fluid flow with boundary conditions. The implementations of this technique are illustrated in Section 4. The error estimate and the results of tables and requires are presented in Section 5 and Section 6 respectively. The discussion and results in Section 7 and the conclusions are written in Section 8.

## 2. Mathematical formulation

Consider the rectilinear unsteady incompressible viscous magneto-hydrodynamic squeezing flow fluid passing in a porous medium among two infinite parallel plates.

The  $\ddot{x}$ -axis is considered the central axis of the channel. Always, the distance between the plates is  $2\delta\ddot{t}$  a part at any time  $\ddot{t}$  with uniform magnetic field  $D = D(0, D_0, 0)$  practiced vertically and is proportional to that act along the  $\ddot{y}$ -axis is perpendicular to the channel. The magnetic field is negligible, for fluid flow the magnetic field is perpendicular and have a constant strength  $\Omega_0$ . Indeed  $D_0 = \Omega_0\ddot{H}_0$ , where  $\ddot{H}_0$  is the magnetic permeability. Moreover, the plate is considered moving symmetrically about the central axis of the canal. The governing equations are the mass conservation and momentum conservation equations for unsteady incompressible squeezing fluid flow can be introduced as [21,22]

$$\frac{\partial \ddot{u}}{\partial \ddot{x}} + \frac{\partial \ddot{v}}{\partial \ddot{y}} = 0,$$

(1)

$$\tilde{\rho} \left( \frac{\partial \ddot{u}}{\partial \ddot{t}} + \ddot{u} \frac{\partial \ddot{u}}{\partial \ddot{x}} + \ddot{v} \frac{\partial \ddot{u}}{\partial \ddot{y}} \right) = -\frac{\partial \ddot{p}}{\partial \ddot{x}} + \nu \left( \frac{\partial^2 \ddot{u}}{\partial \ddot{x}^2} + \frac{\partial^2 \ddot{u}}{\partial \ddot{y}^2} \right) - \sigma D_0^2 \ddot{u} - \frac{\ddot{H}}{k^*} \ddot{u},$$

(2)

$$\tilde{\rho} \left( \frac{\partial \ddot{v}}{\partial \ddot{t}} + \ddot{u} \frac{\partial \ddot{v}}{\partial \ddot{x}} + \ddot{v} \frac{\partial \ddot{v}}{\partial \ddot{y}} \right) = -\frac{\partial \ddot{p}}{\partial \ddot{y}} + \nu \left( \frac{\partial^2 \ddot{v}}{\partial \ddot{x}^2} + \frac{\partial^2 \ddot{v}}{\partial \ddot{y}^2} \right) - \frac{\ddot{H}}{k^*} \ddot{v}.$$

(3)

$\ddot{u}$  and  $\ddot{v}$  are the velocity components in  $\ddot{x}$  and  $\ddot{y}$  direction respectively,  $\tilde{\rho}$  is density,  $\ddot{p}$  is the pressure,  $\nu$  is kinematics viscosity,  $\sigma$  is electric conductivity, and  $k^*$  is constant permeability, the vorticity function can be defined as follows;

$$\ddot{\omega} = \frac{\partial \ddot{v}}{\partial \ddot{x}} - \frac{\partial \ddot{u}}{\partial \ddot{y}},$$

(4)

The generalized pressure as

$$\tilde{p} = \frac{1}{2} \tilde{\rho} (\ddot{u}^2 + \ddot{v}^2) + \ddot{p},$$

(5)

by substituting Equation (4) and Equation (5) into Equations (1)-(3) the above governing equations become as follows:

$$\frac{\partial \ddot{u}}{\partial \ddot{x}} + \frac{\partial \ddot{v}}{\partial \ddot{y}} = 0,$$

(6)

$$\frac{\partial \tilde{p}}{\partial \ddot{x}} + \tilde{\rho} \left( \frac{\partial \ddot{u}}{\partial \ddot{t}} - \ddot{v} \ddot{\omega} \right) = -\nu \frac{\partial \ddot{\omega}}{\partial \ddot{y}} - \sigma D_0^2 \ddot{u} - \frac{\ddot{H}}{k^*} \ddot{u},$$

(7)

$$\frac{\partial \tilde{p}}{\partial \tilde{y}} + \tilde{\rho} \left( \frac{\partial \tilde{v}}{\partial \tilde{t}} - \ddot{u} \ddot{\omega} \right) = -\nu \frac{\partial \ddot{\omega}}{\partial \tilde{x}} - \frac{\tilde{H}}{k^*} \ddot{v}. \quad (8)$$

The simplification of the above system by eliminating the pressure term for Equation (7) and Equation (8) with using Equation (1), yield

$$\tilde{\rho} \left( \frac{\partial \ddot{\omega}}{\partial \tilde{t}} + \ddot{u} \frac{\partial \ddot{\omega}}{\partial \tilde{x}} + \ddot{v} \frac{\partial \ddot{\omega}}{\partial \tilde{y}} \right) = \nu \left( \frac{\partial^2 \ddot{\omega}}{\partial \tilde{x}^2} + \frac{\partial^2 \ddot{\omega}}{\partial \tilde{y}^2} \right) - \sigma D_0^2 \frac{\partial \ddot{u}}{\partial \tilde{y}} - \frac{\tilde{H}}{k^*} \ddot{\omega}, \quad (9)$$

supporting conditions for the problem are as follows:

$$\ddot{u}(\tilde{x}, \tilde{y}, \tilde{t}) = 0, \quad \ddot{v}(\tilde{x}, \tilde{y}, \tilde{t}) = \ddot{v}_w(\ddot{t}), \quad \text{at} \quad \tilde{y} = \delta, \quad (10)$$

$$\ddot{v}(\tilde{x}, \tilde{y}, \tilde{t}) = 0, \quad \frac{\partial \ddot{u}(\tilde{x}, \tilde{y}, \tilde{t})}{\partial \tilde{y}} = 0, \quad \text{at} \quad \tilde{y} = 0. \quad (11)$$

Here,  $\ddot{v}_w(\ddot{t}) = \frac{\partial \delta}{\partial \tilde{t}}$  is the velocity of plates and  $\varepsilon = \frac{\tilde{y}}{\delta(\tilde{t})}$  is dimensionless variable,

the formula for equation (6) and equation (9) can be written as follows:

$$\frac{\partial \ddot{u}}{\partial \tilde{x}} + \frac{\partial \ddot{v}}{\delta(\tilde{t}) \partial \varepsilon} = 0, \quad (12)$$

$$\tilde{\rho} \left( \frac{\partial \ddot{\omega}}{\partial \tilde{t}} + \ddot{u} \frac{\partial \ddot{\omega}}{\partial \tilde{x}} + \ddot{v} \frac{\partial \ddot{\omega}}{\delta(\tilde{t}) \partial \varepsilon} \right) = \nu \left( \frac{\partial^2 \ddot{\omega}}{\partial \tilde{x}^2} + \frac{\partial^2 \ddot{\omega}}{(\delta(\tilde{t}) \partial \varepsilon)^2} \right) - \sigma D_0^2 \frac{\partial \ddot{u}}{\delta(\tilde{t}) \partial \varepsilon} - \frac{\tilde{H}}{k^*} \ddot{\omega}, \quad (13)$$

the functions  $\ddot{u}(\tilde{x}, \tilde{y}, \tilde{t})$  and  $\ddot{v}(\tilde{x}, \tilde{y}, \tilde{t})$  of the boundary conditions are:

$$\ddot{u}(\tilde{x}, \varepsilon, \tilde{t}) = 0, \quad \ddot{v}(\tilde{x}, \varepsilon, \tilde{t}) = \ddot{v}_w(\ddot{t}), \quad \text{at} \quad \varepsilon = 1, \quad (14)$$

$$\ddot{u}(\tilde{x}, \varepsilon, \tilde{t}) = 0, \quad \frac{\partial \ddot{u}(\tilde{x}, \varepsilon, \tilde{t})}{\partial \varepsilon} = 0, \quad \text{at} \quad \varepsilon = 0, \quad (15)$$

the velocity components can be referred to as:

$$\ddot{u} = \frac{k^* - \tilde{x}}{\delta(\tilde{t})} \ddot{v}_w(\ddot{t}) \frac{\partial h(\varepsilon)}{\partial \varepsilon}, \quad \ddot{v} = \ddot{v}_w(\ddot{t}) h(\varepsilon), \quad \ddot{\omega} = -\frac{k^* - \tilde{x}}{\delta(\tilde{t})^2} \ddot{v}_w(\ddot{t}) \frac{\partial^2 h(\varepsilon)}{\partial \varepsilon^2}, \quad (16)$$

Substituting Equation (16) into Equation (12) and Equation (13), with simplification yields;



$$\frac{d^4h(\varepsilon)}{d\varepsilon^4} - \frac{\delta\ddot{v}_w}{\nu} \left( h(\varepsilon) \frac{d^3h(\varepsilon)}{d\varepsilon^3} - \frac{dh(\varepsilon)}{d\varepsilon} \frac{d^2h(\varepsilon)}{d\varepsilon^2} - \varepsilon \frac{d^3h(\varepsilon)}{d\varepsilon^3} - 2 \frac{d^2h(\varepsilon)}{d\varepsilon^2} \right) - \frac{\delta^2}{\nu \ddot{v}_w} \frac{d\ddot{v}_w}{d\ddot{t}} \frac{d^2h(\varepsilon)}{d\varepsilon^2} - M_G \frac{d^2h(\varepsilon)}{d\varepsilon^2} - M_P \frac{d^2h(\varepsilon)}{d\varepsilon^2} = 0, \quad (17)$$

$M_G$  is the magnetic-hydrodynamic parameter and  $M_P$  is porous parameter, the boundary condition can be defined by the Equation (14) and Equation (15) as follows;

$$h(1) = 1, \quad \frac{dh(1)}{d\varepsilon} = 0, \quad h(0) = 0, \quad \frac{d^2h(0)}{d\varepsilon^2} = 0. \quad (18)$$

Thus, the value of Reynolds number from the similarity solution can introduce the following:

$$\frac{\delta\ddot{v}_w}{\nu} = R_E, \quad \frac{\delta^2}{\nu \ddot{v}_w} \frac{d\ddot{v}_w}{d\ddot{t}} = R_E Q, \quad (19)$$

Here,  $R_E$  and  $Q$  are functions of  $\ddot{t}$ , which are taken to be constants for the similarity solution, if we integrate the equation  $\frac{\delta\ddot{v}_w}{\nu} = R_E$ , we get;

$$\delta(\ddot{t}) = \sqrt{2\nu R_E \ddot{t} + \delta_0^2}, \quad (20)$$

$2\delta_0$  is the distance between the two plates at time  $t = 0$ . Two cases in which the motion of the plates can be described independently of the Reynolds number can be listed as follows:

- $R_E > 0$ : The plates move apart symmetrically with respect to  $\varepsilon = 0$  or  $\ddot{y} = 0$ .
- $R_E < 0$ : The plates come close together and there is pressure flow exists with similar velocity profiles as long as  $\delta(\ddot{t}) > 0$ .

By using Equation (13) and Equation (14), Assuming that  $Q = -1$ , then Equation (17) can be written as;

$$\frac{d^4h(\varepsilon)}{d\varepsilon^4} - R_E \left( h(\varepsilon) \frac{d^3h(\varepsilon)}{d\varepsilon^3} - \frac{dh(\varepsilon)}{d\varepsilon} \frac{d^2h(\varepsilon)}{d\varepsilon^2} - \varepsilon \frac{d^3h(\varepsilon)}{d\varepsilon^3} - 3 \frac{d^2h(\varepsilon)}{d\varepsilon^2} \right) - M_G \frac{d^2h(\varepsilon)}{d\varepsilon^2} - M_P \frac{d^2h(\varepsilon)}{d\varepsilon^2} = 0, \quad (21)$$

The boundary conditions of Equation (18) can be described according to the following cases:

- No slip:  $h(1) = 1, \quad \frac{dh(1)}{d\varepsilon} = 0,$   
(22)
- Slip:  $h(1) = 1, \quad \frac{dh(1)}{d\varepsilon} = \vartheta \frac{d^2h(1)}{d\varepsilon^2},$   $\vartheta$  is the slip parameter.  
(23)

### 3. The Basic Rules of Perturbation Iteration Technique [19, 20]

The nonlinear ordinary differential equation can be considered for  $h(\varepsilon)$  as follows;

$$\ddot{G}\left(h(\varepsilon), \frac{dh(\varepsilon)}{d\varepsilon}, \frac{d^2h(\varepsilon)}{d\varepsilon^2}, \frac{d^3h(\varepsilon)}{d\varepsilon^3}, \dots, \frac{d^{(n-1)}h(\varepsilon)}{d\varepsilon^{(n-1)}}, \frac{d^{(n)}h(\varepsilon)}{d\varepsilon^{(n)}}\right) = 0, \quad (24)$$

$\ddot{G}$  is a function on  $h(\varepsilon)$  with its derivatives,  $h(\varepsilon)$  is an unknown; and  $\varepsilon$  is a dependent variable. In Equation (24), can addition auxiliary perturbation parameter  $\gamma$  as shown in the equation following;

$$\ddot{G}(h(\varepsilon), h'(\varepsilon), h''(\varepsilon), \dots, h^{(n-1)}(\varepsilon), h^{(n)}(\varepsilon), \gamma) = 0, \quad (25)$$

Equation (25) can be rewritten as the following;

$$\ddot{G}(h_{m+1}(\varepsilon), h'_{m+1}(\varepsilon), h''_{m+1}(\varepsilon), h'''_{m+1}(\varepsilon), \dots, h^{(n-1)}_{m+1}(\varepsilon), h^{(n)}_{m+1}(\varepsilon), \gamma) = 0, \quad (26)$$

where  $m$  represents the  $m^{\text{th}}$  iteration with defined perturbation expansions with correction term as follows;

$$\begin{aligned} h_1 &= h_0 + \gamma(h_c)_0, \\ h_2 &= h_1 + \gamma(h_c)_1, \\ h_3 &= h_2 + \gamma(h_c)_2, \\ &\vdots \\ h_{m+1} &= h_m + \gamma(h_c)_m, \end{aligned} \quad (27)$$

where  $\gamma$  is the parameter of small perturbation and in the perturbation expansion  $h_c$  is the correction term. Subsequently, substituting Equation (27) in Equation (26), yield

$$\ddot{G}(h_m(\varepsilon) + \gamma(h_c)_m, h'_m(\varepsilon) + \gamma(h_c)'_m, h''_m(\varepsilon) + \gamma(h_c)''_m, \dots, h^{(n)}_m(\varepsilon) + \gamma(h_c)^{(n)}_m, \gamma) = 0, \quad (28)$$

Now, taking the Taylor series expansion in the next step for the first-order derivative in the neighborhood when  $\gamma = 0$ , yields

$$\begin{aligned} \ddot{G}\left(h(\varepsilon), \frac{dh_m(\varepsilon)}{d\varepsilon}, \frac{d^2h_m(\varepsilon)}{d\varepsilon^2}, \dots, \frac{d^{(n)}h_m(\varepsilon)}{d\varepsilon^{(n)}}, 0\right) &+ \gamma \frac{d\ddot{G}}{dh_m} \cdot (h_c)_m \Big|_{\gamma=0} + \gamma \frac{d\ddot{G}}{dh'_m} \cdot (h_c)'_m \Big|_{\gamma=0} + \dots + \\ &\gamma \frac{d\ddot{G}}{dh^{(n-1)}_m} \cdot (h_c)^{(n-1)}_m \Big|_{\gamma=0} + \gamma \frac{d\ddot{G}}{dh^{(n)}_m} \cdot (h_c)^{(n)}_m \Big|_{\gamma=0}. \end{aligned} \quad (29)$$

By calculating all derivatives at  $\gamma = 0$ , the results in Equation (29) get an ordinary differential equation. The resulting equation is solved with the assistance of the boundary condition and initial condition to obtain  $(h_c)_m(\varepsilon)$ . The value of  $(h_c)_m(\varepsilon)$  is substituted in Equation (27) to obtain the  $h_{m+1}(\varepsilon)$ . It is the approximate analytical solution; it is in the form of power series.

Thus, we can express the approximate solutions in the following way, firstly can be defined:

$$h_0 = C_0, \quad (h_c)_m = C_{m+1}, \quad (30)$$

and the other solutions can be defined in the following iterations

$$\begin{aligned} h_0 &= C_0, \\ h_1 &= h_0 + (h_c)_0 = C_0 + C_1, \\ h_2 &= h_1 + (h_c)_1 = C_0 + C_1 + C_2, \\ &\vdots \\ h_{m+1} &= h_m + (h_c)_m = C_0 + C_1 + C_2 + \dots + C_{m+1} = \sum_{i=0}^{m+1} C_i, \end{aligned} \quad (31)$$

consequently, the value of  $(h_c)_{m+1}$  are substituted in Equation (27) to obtain on  $h_m(\varepsilon)$ . It is the approximate-analytical solution required, which is in the form of the power series. The solution to Equation (24) can be represented as:

$$h(\varepsilon) = \lim_{m \rightarrow \infty} h_{m+1} = \sum_{i=0}^{\infty} C_i, \quad (32)$$

#### 4. Implementations of Unsteady Viscous Squeezing Flow Fluid Problem

To obtain an approximate analytical solution for a non-linear differential equation, PIT (1,1) will be applied to solve Equation (21). Consider the following equation

$$\ddot{G} \left( h(\varepsilon), \frac{dh(\varepsilon)}{d\varepsilon}, \frac{d^2h(\varepsilon)}{d\varepsilon^2}, \frac{d^3h(\varepsilon)}{d\varepsilon^3}, \frac{d^4h(\varepsilon)}{d\varepsilon^4}, \gamma \right) = \frac{d^4h(\varepsilon)}{d\varepsilon^4} - \gamma R_E \left( h(\varepsilon) \frac{d^3h(\varepsilon)}{d\varepsilon^3} - \frac{dh(\varepsilon)}{d\varepsilon} \frac{d^2h(\varepsilon)}{d\varepsilon^2} - \varepsilon \frac{d^3h(\varepsilon)}{d\varepsilon^3} - 3 \frac{d^2h(\varepsilon)}{d\varepsilon^2} \right) - \gamma M_G \frac{d^2h(\varepsilon)}{d\varepsilon^2} - \gamma M_P \frac{d^2h(\varepsilon)}{d\varepsilon^2} = 0, \quad (33)$$

The perturbation expansion with correction term is defined as:

$$h_{m+1} = h_m + \gamma(h_c)_m, \quad (34)$$

$m$  is  $m^{\text{th}}$  iteration,  $h_c$  is correction term in perturbation expansion. Through compensation Equation (34) into Equation (33) and expanding the resulting equations in a Taylor series expansion for the first derivative terms about  $\gamma = 0$ ,

$$\begin{aligned} &\ddot{G} \left( h_m(\varepsilon), \frac{dh_m(\varepsilon)}{d\varepsilon}, \frac{d^2h_m(\varepsilon)}{d\varepsilon^2}, \frac{d^3h_m(\varepsilon)}{d\varepsilon^3}, \frac{d^4h_m(\varepsilon)}{d\varepsilon^4}, 0 \right) + \gamma \frac{d\ddot{G}}{dh_m} \cdot (h_c)_m \Big|_{\gamma=0} + \\ &\gamma \frac{d\ddot{G}}{dh_m''} \cdot (h_c)''_m \Big|_{\gamma=0} + \\ &\gamma \frac{d\ddot{G}}{dh_m'''} \cdot (h_c)'''_m \Big|_{\gamma=0} + \gamma \frac{d\ddot{G}}{dh_m''''} \cdot (h_c)''''_m \Big|_{\gamma=0} + \ddot{G}_\gamma = 0, \end{aligned} \quad (35)$$

where,

$$\ddot{G}(h_m, h'_m, h''_m, h'''_m, h''''_m, \gamma) = h''''_m - \gamma R_E [h_m h'''_m - h'_m h''_m - \varepsilon h'''_m - 3h''_m] - \gamma M_G h''_m - \gamma M_P h''_m$$

$$\ddot{G}(h_m, h'_m, h''_m, h'''_m, h''''_m, 0) = h''''_m,$$

$$\ddot{G}_{h_m} = -\gamma R_E h'''_m, \ddot{G}_{h'_m} = \gamma R_E h''_m, \ddot{G}_{h''_m} = -\gamma R_E h'_m + 3\gamma R_E - \gamma M_G - \gamma M_P$$

(36)

$$\ddot{G}_{h'''_m} = -\gamma R_E h_m + \gamma R_E \varepsilon, \ddot{G}_{h''''_m} = 1$$

$$\ddot{G}_\gamma = R_E [h_m h'''_m - h'_m h''_m - \varepsilon h'''_m - 3h''_m] - M_G h''_m - M_P h''_m.$$

Compensating Equation (36) in Equation (35), the result is the following equation:

$$(h_c)'''_m = -\frac{1}{\gamma} h''''_m(\varepsilon) - R_E [h_m h'''_m - h'_m h''_m - \varepsilon h'''_m - 3h''_m] - M_G h''_m - M_P h''_m.$$

(37)

Subject to the initial condition:

$$h_0(\varepsilon) = \Delta_0 + \Delta_1 \varepsilon + \frac{1}{2!} \Delta_2 \varepsilon^2 + \frac{1}{3!} \Delta_3 \varepsilon^3,$$

which,

$$h(0) = \Delta_0, \quad \frac{dh(0)}{d\varepsilon} = \Delta_1, \quad \frac{d^2h(0)}{d\varepsilon^2} = \Delta_2, \quad \frac{d^3h(0)}{d\varepsilon^3} = \Delta_3,$$

Now, the preliminary condition obtained for the proposed problem contains constants  $\Delta_1$  and  $\Delta_3$  are unknown. The obtained approximate analytical solutions of Equation (21) at  $\varepsilon = 1$  can be utilized to extract the values of the constants  $\Delta_1$  and  $\Delta_3$ . The approximate analytical solutions to the governing equation of this problem are obtained by subtract the iteration solutions as:

$$h_0(\varepsilon) = \Delta_1 \varepsilon + \frac{1}{3!} \Delta_3 \varepsilon^3,$$

$$h_1(\varepsilon) = \Delta_1 \varepsilon + \frac{1}{6} \Delta_3 \varepsilon^3 - 0.2(-0.04166666667 \Delta_3 M_P + 0.1666666667 \Delta_3 R_E - 0.04166666667$$

$$M_G \Delta_3) \varepsilon^5 - 0.0003968253968 \Delta_3^2 R_E \varepsilon^7,$$

$$h_2(\varepsilon) = \Delta_1 \varepsilon + 0.16666666667 \Delta_3 \varepsilon^3 + 0.008333333333 M_P \Delta_3 - 0.03333333333 R_E \Delta_3 - 0.008333$$

$$M_G \Delta_3) \varepsilon^5 + (-0.0003968253967 R_E \Delta_3^2 + 0.004761904766 R_E^2 \Delta_3 + 0.0001984126985 M_G^2 \Delta_3 +$$

$$0.0001984126985 \Delta_3 M_P^2 + 0.0003968253970 R_E \Delta_1 \Delta_3 M_P + 0.0003968253970 R_E \Delta_1 M_G \Delta_3 -$$

$$0.001587301588 \Delta_1 \Delta_3 R_E^2 - 0.001984126985 R_E M_P \Delta_3 - 0.001984126985 \Delta_3 R_E M_G +$$

$$0.0003968253970 M_G M_P \Delta_3) \varepsilon^7 + (0.00008818342160 \Delta_3^2 R_E^2 - 0.00002204585540 \Delta_1 \Delta_3^2 R_E^2 -$$

$$0.000016533439154 \Delta_3^2 M_P R_E - 0.00001653439154 \Delta_3^2 M_G R_E) \varepsilon^9 + (-4.008337343 10^{-7} \Delta_3^3 R_E^2$$

$$-0.000005611672290 \Delta_3^3 R_E - 7.014590351 10^{-7} \Delta_3^3 R_E M_P M_G + 0.000002805836142 R_E^2 M_P$$

$$\Delta_3^3 + 0.000002805836142 \Delta_3^3 M_G R_E^2 - 3.507295177 10^{-7} \Delta_3^3 M_G^2 R_E^2) \varepsilon^{11} + (-6.16667283310^{-8}$$

$$\Delta_3^3 R_E^2 + 1.541668209 10^{-8} \Delta_3^3 R_E^2 M_P + 1.541668209 10^{-8} \Delta_3^3 R_E^2 M_G) \varepsilon^{13} - 4.037702454 10^{-10}$$

$$\Delta_3^4 R_E^3 \varepsilon^{15}.$$

⋮

## 5. The Convergence of Perturbation Iteration Technique



In this section, we have applied the theorems in [19,20] to find the error estimate of the solutions of PIT. If there exists  $0 < \varpi_i < 1$  then  $\|\bar{\Pi}_{i+1}\| \leq \varpi_i \|\bar{\Pi}_i\|, i = 0,1,2, \dots$ , is the condition of convergent can be define the iteration solutions as follows:

$$\begin{aligned} \bar{\Pi}_0 &= h_0, \\ \bar{\Pi}_0 + \bar{\Pi}_1 &= h_0 + (h_c)_0, \\ \bar{\Pi}_0 + \bar{\Pi}_1 + \bar{\Pi}_2 &= h_0 + (h_c)_0 + (h_c)_1, \\ &\vdots \\ \bar{\Pi}_0 + \bar{\Pi}_1 + \bar{\Pi}_2 + \dots + \bar{\Pi}_n &= h_0 + (h_c)_0 + (h_c)_1 + \dots + (h_c)_n. \end{aligned}$$

All solutions are achieved for the condition of convergence in Table.1 and Table.2 as follows:

**Table.1.** The values of convergence for no slip at boundaries condition when  $M_G=0.8$  and  $M_P=0.9$ .

$\varpi_{i\ \infty}$	$R_E = 0.3$	$R_E = 0.5$	$R_E=1$	$R_E=1.5$	$R_E=1.7$	$R_E=2$
$\varpi_0$	0.007954036	0.007954036	0.045915634	0.101981303	0.129956214	0.179438351
$\varpi_1$	0.018843771	0.004857429	0.028212776	0.057655831	0.068045175	0.081629464
$\varpi_2$	0.015039955	0.009833667	0.005456368	0.009067662	0.011342190	0.016042820
$\vdots$	$\vdots$	$\vdots$	$\vdots$	$\vdots$	$\vdots$	$\vdots$

**Table.٢.** The values of convergence for slip at boundaries conditions when  $R_E = 1.2, M_G = 0.9$  and  $M_P = 0.8$ .

$\varpi_{i\ \infty}$	$\vartheta = 0.01$	$\vartheta = 0.05$	$\vartheta = 0.10$	$\vartheta = 0.15$	$\vartheta = 0.20$	$\vartheta = 0.25$
$\varpi_0$	0.067225515	0.07156901	0.07794501	0.085758276	0.095762845	0.109942952
$\varpi_1$	0.039693595	0.03598351	0.02993378	0.021327814	0.007761666	0.019093009
$\varpi_2$	0.008618831	0.00861883	0.01211964	0.019660893	0.056638598	0.065330735
$\vdots$	$\vdots$	$\vdots$	$\vdots$	$\vdots$	$\vdots$	$\vdots$

From Table (1) and Table (2), we can see that the series of approximate analytical solutions of  $h(\varepsilon)$  are convergent.

## 6. Discussions and results

A similarity solutions of unsteady squeezing flow of a viscous magneto-hydrodynamic fluid passing through porous medium between two infinite parallel plates reducing and approaching for each other under the impact of an electromagnetic field with slip and no slip at the boundaries has been presented under the influence of different values for the physical parameters Reynolds number  $R_E$ , slip parameter  $\vartheta$ , magnetic-hydrodynamic parameter  $M_G$  and porous parameter  $M_P$  on the normal velocity  $h(\varepsilon)$  and longitudinal velocity  $h'(\varepsilon)$ . This solution exists only when the distance between the plates varies and the squeezing flow takes place for  $R_E > 0$ . Table (3) and Table(4) presented the convergence of values  $\Delta_1$  and  $\Delta_3$  for different values of the emerging parameters. Tables (5)-(8) displayed comparison between the results presented, RKF5 and HPM, we can note that the solutions are well matched. These tables show that the solutions resulting from the proposed method are closer to the numerical solution than the method by calculating

the percentage error. Also, the comparison of the presented solution with RK4 offered in Table (9). From these tables, we find that the solutions are compatible to at least five decimal places.

**Table.3.** The computed values of  $\Delta 1$  and  $\Delta 3$  when  $\vartheta = 0.9, M_G = 1,$

	$R_E = 0.5, M_P = 0.8$		$R_E = 0.3, M_P = 0.5$	
	$\Delta 1$	$\Delta 3$	$\Delta 1$	$\Delta 3$
Order1	0.69023771	1.88160453	0.7161690113	1.679804397
Order2	0.69076316	1.87810659	0.7162295914	1.679385211
Order3	0.69075475	1.87816078	0.7162296540	1.679384833
Order4	0.69075484	1.87816019	0.7162296538	1.679384833

**Table.4.** The computed values of  $\Delta 1$  and  $\Delta 3$  when  $\vartheta = 0.9, M_G = 0.9,$

	$R_E = 0.3, M_P = 0.9$		$R_E = 0.6, M_P = 1$	
	$\Delta 1$	$\Delta 3$	$\Delta 1$	$\Delta 3$
Order1	0.728099396	1.58563057	0.671348183	2.0285017
Order2	0.728640645	1.58202702	0.673600781	2.0132738
Order3	0.728645718	1.58199543	0.673540798	2.0136653
Order4	0.728645738	1.58199531	0.673541863	2.0136584

**Table 5.** The compared solutions between RKF5, HPM, and the present solutions

$\vartheta = 0, R_E = 0.5, M_G = 1, M_P = 0.7$			
$\varepsilon$	RKF5[22]	HPM [22]	Present solutions
0.0	0.000000	0.000000	0.000000
0.1	0.149891	0.149891	0.149891
0.2	0.296726	0.296726	0.296726
0.3	0.347456	0.347456	0.437456
0.4	0.569050	0.569050	0.569050
0.5	0.688501	0.688500	0.688500
0.6	0.792825	0.792825	0.792825
0.7	0.879069	0.879068	0.879068
0.8	0.944296	0.944296	0.944295
0.9	0.985583	0.985583	0.985582
1.0	1.000000	1.000000	1.000000

**Table 6.** Comparison between RKF5, HPM, and present solutions

$\vartheta = 0, R_E = 1, M_G = 1, M_P = 0.3$					
$\varepsilon$	RKF5[22]	HPM [22]	Percentage error	Present solutions	Percentage error

0.0	0.000000	0.000000	0.000000	0.000000	0.000000
0.1	0.156416	0.156262	0.000984	0.156416	0.000000
0.2	0.308960	0.308676	0.000919	0.308960	0.000000
0.3	0.453866	0.453849	0.000037	0.453866	0.000000
0.4	0.587568	0.587161	0.000692	0.587568	0.000000
0.5	0.706796	0.706409	0.000547	0.706796	0.000000
0.6	0.808646	0.808327	0.000394	0.808646	0.000000
0.7	0.890646	0.890426	0.000247	0.890646	0.000000
0.8	0.950797	0.950682	0.000120	0.950797	0.000000
0.9	0.987588	0.987555	0.000033	0.987588	0.000000
1.0	1.000000	1.000000	0.000000	1.000000	0.000000

**Table 7.** Comparison between RKF5, HPM, and present solution

$\vartheta = 0.9$ $R_E = 0.5,$ $M_G = 1,$ $M_P = 0.8$					
$\varepsilon$	RKF5[22]	HPM [22]	Percentage error	Present solution	Percentage error
0.0	0.000000	0.000000	0.000000	0.000000	0.000000
0.1	0.069388	0.069393	0.000072	0.069388	0.000000
0.2	0.140654	0.140663	0.000063	0.140654	0.000000
0.3	0.215670	0.215683	0.000060	0.215670	0.000000
0.4	0.296303	0.296317	0.000047	0.296302	0.000000
0.5	0.384403	0.384419	0.000041	0.384402	0.000000
0.6	0.481805	0.481821	0.000033	0.481804	0.000000
0.7	0.590316	0.590331	0.000025	0.590316	0.000000
0.8	0.711710	0.711721	0.000015	0.711710	0.000000
0.9	0.847715	0.847721	0.000007	0.847715	0.000000
1.0	1.000000	1.000000	0.000000	1.000000	0.000000

**Table 8.** Comparison between RKF5, HPM, and present solution

$\vartheta = 0.9$ $R_E = 0.3,$ $M_G = 0.9,$ $M_P = 0.9$					
$\varepsilon$	RKF5[22]	HPM[22]	Percentage error	Present solutions	Percentage error
0.0	0.000000	0.000000	0.000000	0.000000	0.000000
0.1	0.073128	0.073117	0.000150	0.073128	0.000000
0.2	0.147841	0.147820	0.000142	0.147841	0.000000
0.3	0.225732	0.225703	0.000128	0.225732	0.000000
0.4	0.308414	0.308379	0.000113	0.308413	0.000000
0.5	0.397527	0.397490	0.000093	0.397526	0.000000
0.6	0.494748	0.494712	0.000072	0.494748	0.000000
0.7	0.601801	0.601770	0.000051	0.601800	0.000000
0.8	0.720459	0.720436	0.000031	0.720459	0.000000
0.9	0.852559	0.852546	0.000015	0.852559	0.000000
1.0	1.000000	1.000000	0.000000	1.000000	0.000000

**Table 9.** Comparison between RK4 and present solution for  $R_E = 1.2, M_G = 0.5$  and  $M_P = 0.7$ .

$\varepsilon$	Nonslip boundary condition			Slip boundary condition		
	RK4	PIA	Percentage error	RK4	PIA	Percentage error
0.1 $10^{-5}$	0.1639339193	0.1639358808	$1.18 \times 10^{-5}$	0.1797439794	0.1797464214	$1.3 \times 10^{-5}$
0.2 $10^{-5}$	0.3230159819	0.3230197645	$1.17 \times 10^{-5}$	0.3534471809	0.3534518854	$1.3 \times 10^{-5}$
0.3 $\times 10^{-5}$	0.4726255618	0.4726307448	$1.0 \times 10^{-5}$	0.5153564530	0.5153628891	1.2
0.4 $\times 10^{-5}$	0.6085905509	0.6085964690	$9.7 \times 10^{-6}$	0.6602757609	0.6602830917	1.1
0.5 $10^{-6}$	0.7273783495	0.7273841513	$7.9 \times 10^{-6}$	0.7838014283	0.7838085869	$9.1 \times 10^{-6}$
0.6 $10^{-6}$	0.8262491853	0.8262539094	$5.7 \times 10^{-6}$	0.8825083556	0.8825141394	$6.5 \times 10^{-6}$
0.7 $10^{-6}$	0.9033628521	0.9033655149	$2.9 \times 10^{-6}$	0.9540756917	0.9540788677	$6.6 \times 10^{-6}$
0.8 $10^{-7}$	0.9578329141	0.9578326272	$2.9 \times 10^{-7}$	0.9973444250	0.9973438119	$6.1 \times 10^{-7}$
0.9 $\times 10^{-6}$	0.9897258818	0.9897221041	$3.8 \times 10^{-6}$	1.0123040820	1.0122986240	5.3

**The no slip boundary:** For the fixed positive  $M_G$  and  $M_P$ , the growing values of  $R_E$  lead to increase of the normal velocity for  $\varepsilon = 0$  to  $\varepsilon = 1$ . The longitudinal velocity is increase for  $0 \leq \varepsilon < 0.45$  but occurs opposite for  $0.45 \leq \varepsilon < 1$ . The behavior of fluid flow of  $M_G$  and  $M_P$  is similar can be seen in Figure (2) and Figure (3) given the decrease of normal velocity with rising  $M_G$  and  $M_P$  respectively for the fixed positive  $R_E$ . Further, The longitudinal velocity is decrease for  $0 \leq \varepsilon < 0.45$  but occurs inverse for  $0.45 \leq \varepsilon < 1$ .

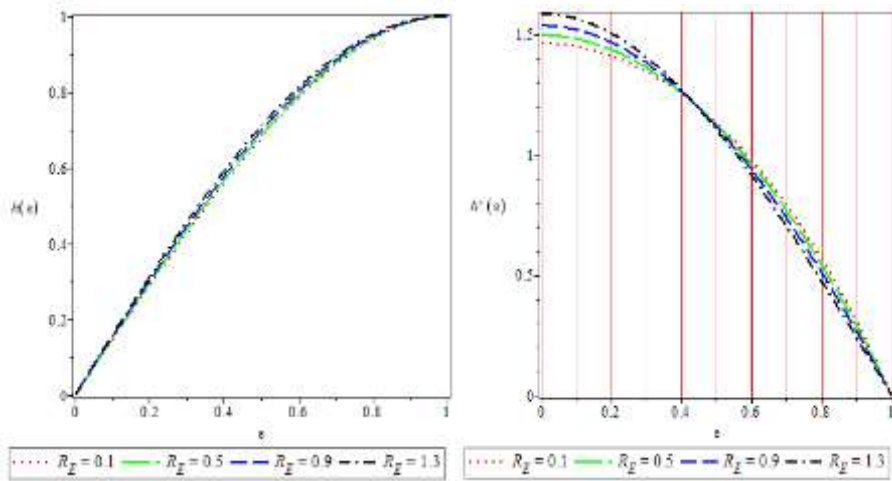


Figure.1. The variation of  $R_E$  for  $M_G = 1$ ,  $M_P = 1$  and  $\vartheta = 0$ .

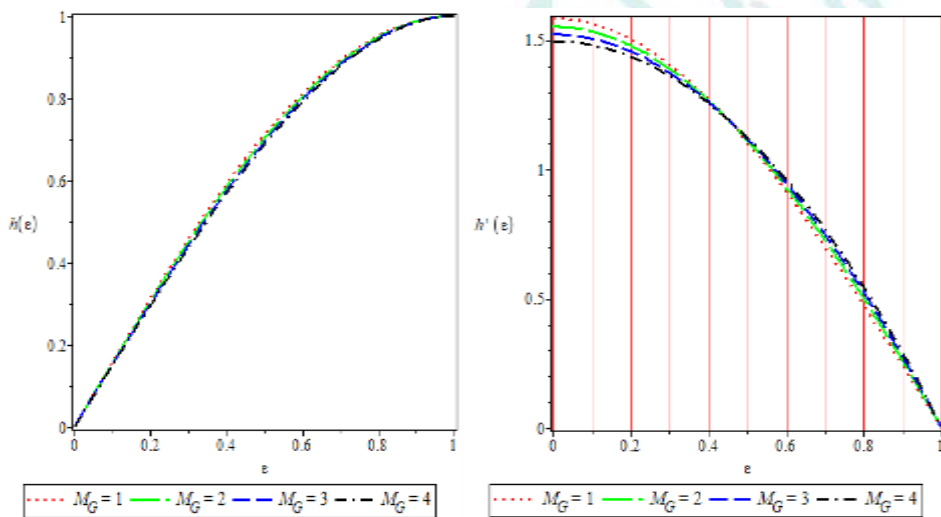


Figure.2. The variation of  $M_G$  for  $R_E = 1.3$ ,  $M_P = 1$  and  $\vartheta = 0$ .



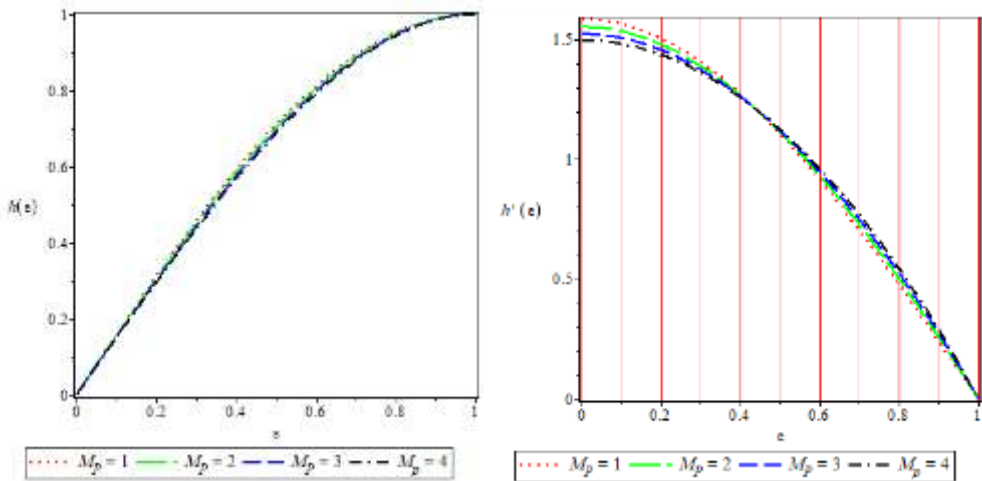


Figure.3. The variation of  $M_p$  for  $R_E = 1.3$ ,  $M_G = 1$  and  $\vartheta = 0$ .

**The slip boundary:** For the fixed positive  $M_G$  and  $M_p$ , the raising values of  $R_E$  lead to decrease of the normal velocity for  $\varepsilon = 0$  to  $\varepsilon = 1$ . The longitudinal velocity is decrease for  $0 \leq \varepsilon < 0.55$  but occurs opposite for  $0.55 \leq \varepsilon < 1$ . The behavior of fluid flow of  $\vartheta, M_G$  and  $M_p$  is similar can be seen in Figures (5)-(7) given the decrease of normal velocity and  $M_p$  respectively for the fixed positive  $R_E$ . Further, The longitudinal velocity is decrease for  $0 \leq \varepsilon < 0.55$  but occurs opposite for  $0.55 \leq \varepsilon < 1$ .

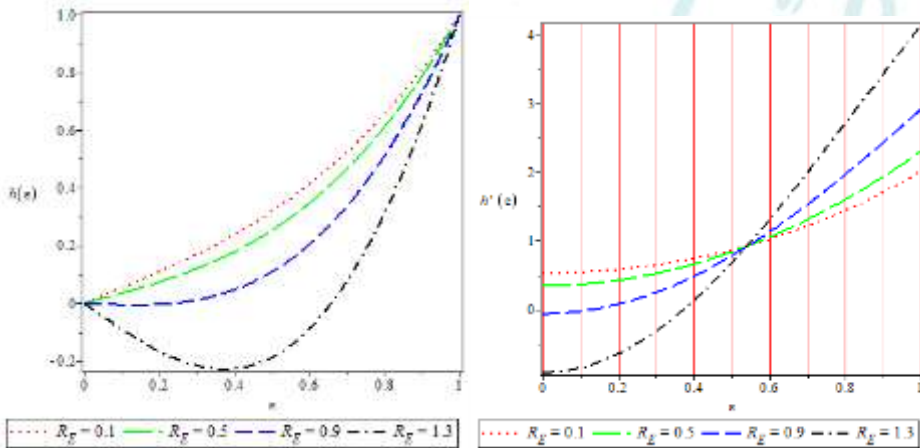


Figure.4. The variation of  $R_E$  for  $M_G = 1$ ,  $M_p = 1$  and  $\vartheta = 0.6$ .

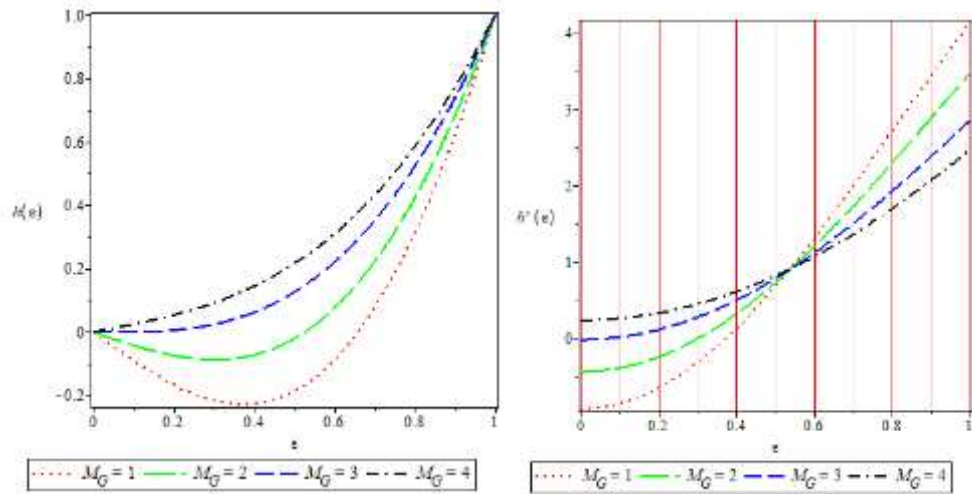


Figure.5. The variation of  $M_G$  for  $R_E = 1.3$ ,  $M_P = 1$  and  $\vartheta = 0.6$ .

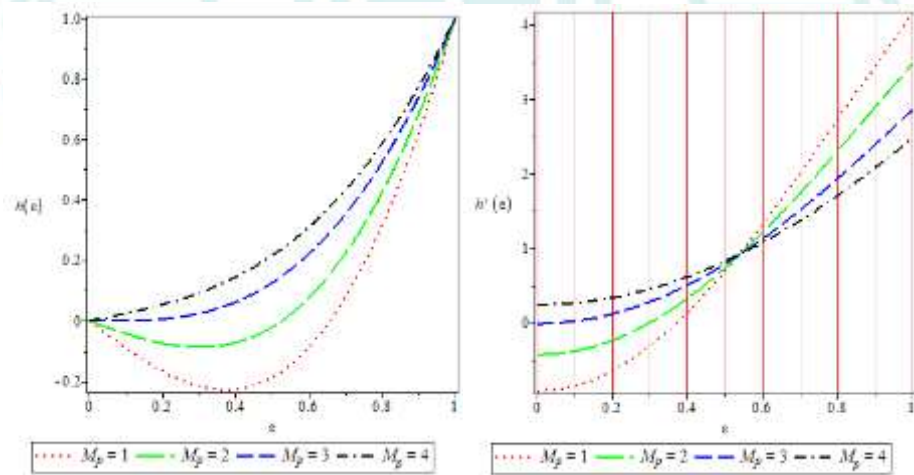


Figure.6. The variation of  $M_P$  for  $R_E = 1.3$ ,  $M_G = 1$  and  $\vartheta = 0.6$ .

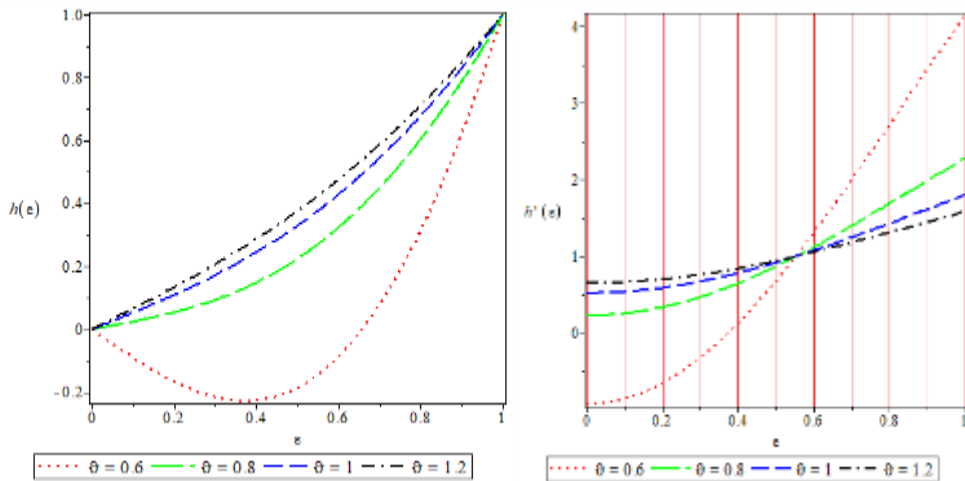


Figure.7. The variation of  $\vartheta$  for  $R_E = 1.3$ ,  $M_G = 1$  and  $M_P = 1$ .

Obviously, Figure (8) and Figure (9) indicated to an effect of  $R_E$ ,  $M_G$  and  $M_P$  on the generalized pressure  $\tilde{p}$  for both slip and no slip boundary conditions. This effect is similar to both cases of increasing  $\tilde{p}$  at higher  $R_E$  rising and the decreasing generalized pressure at increasing  $M_G$  and  $M_P$ .

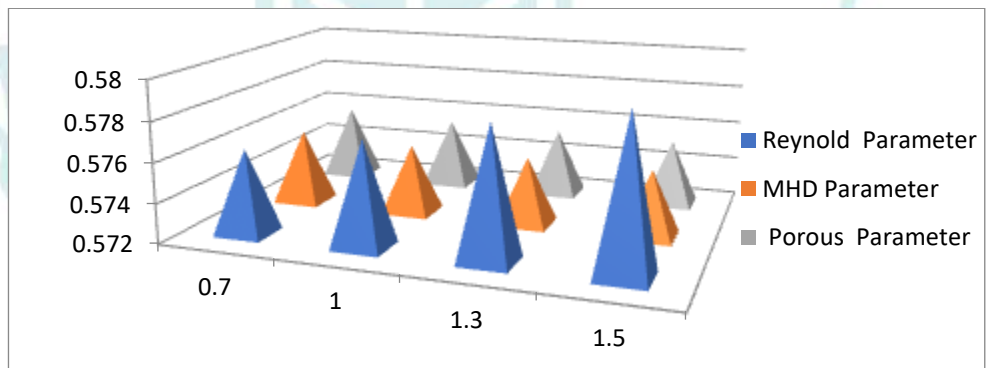


Figure.8. The behavior of the generalized pressure  $\tilde{p}$  for  $R_E = 0.5$ ,  $M_G = 0.6$ ,  $\vartheta = 0.6$  and  $M_P = 0.6$ .

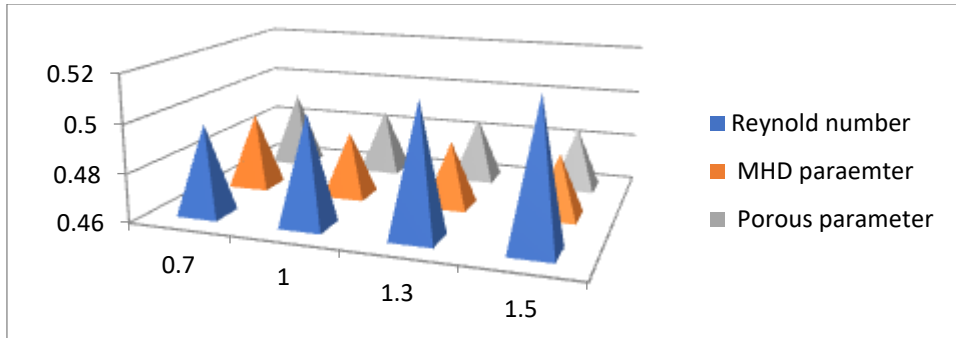
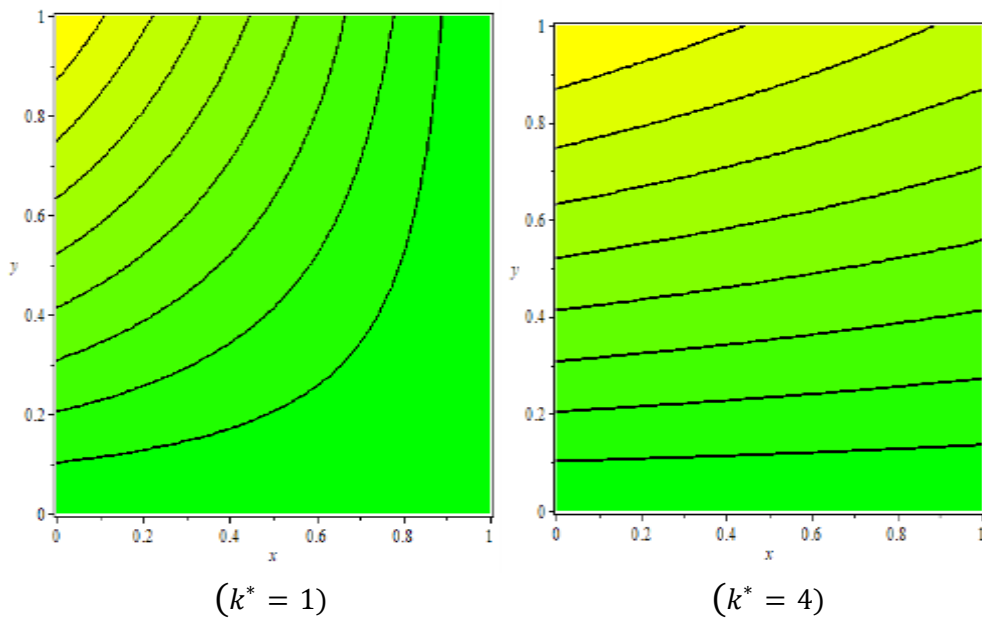


Figure.9. The behavior of the generalized pressure  $\tilde{p}$  for  $R_E = 0.5$ ,  $M_G = 0.6$ ,  $\vartheta = 0$  and  $M_p = 0.6$ .

Vorticity is useful for understanding potential flow solutions can be perturbed to model flows. In general, the presence of viscosity causes a diffusion of vorticity away from the vortex cores into flow field. This flow is accounted by a diffusion term in the vorticity transport equation. The results of the vorticity function with  $k^* = 1, 4, 10, 20$  are depicted in Figure (10) and Figure (11) for slip and no slip at boundaries conditions. These numbers show that the form of flow function are curves that do not intersect with increasing constant permeability  $k^*$  but when this constant is increased the curves turn into straight lines.



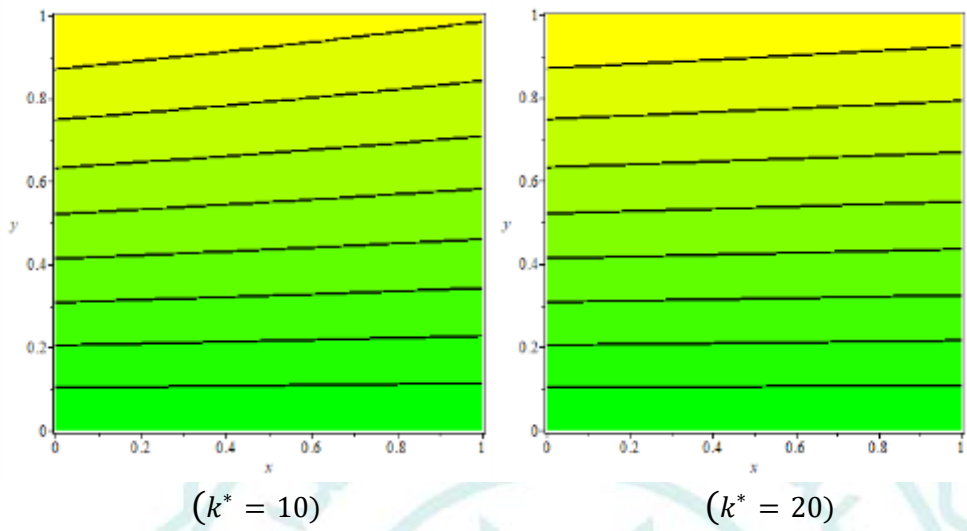
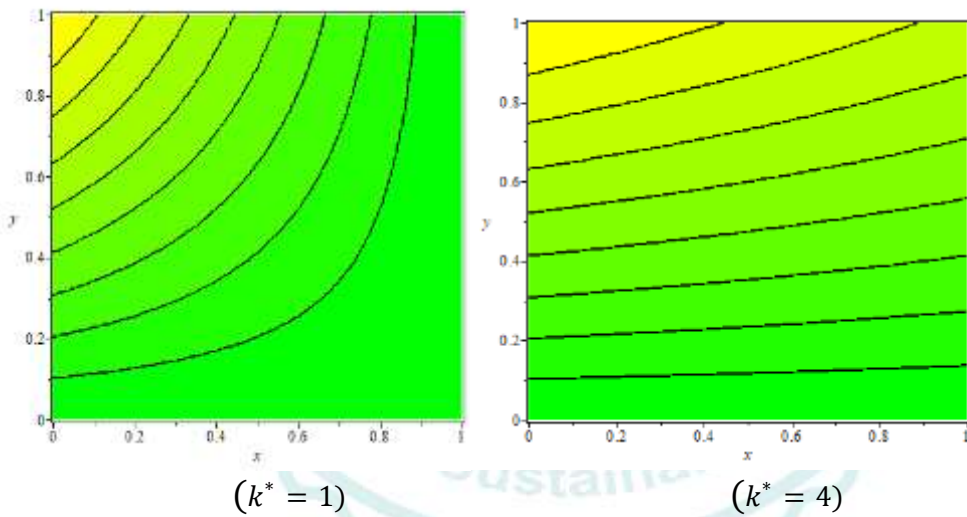


Figure.10. The counter of the vorticity function for  $R_E = 1.5$ ,  $M_G = 0.5$ ,  $\vartheta = 0.1$ , and  $M_P = 0.7$ .





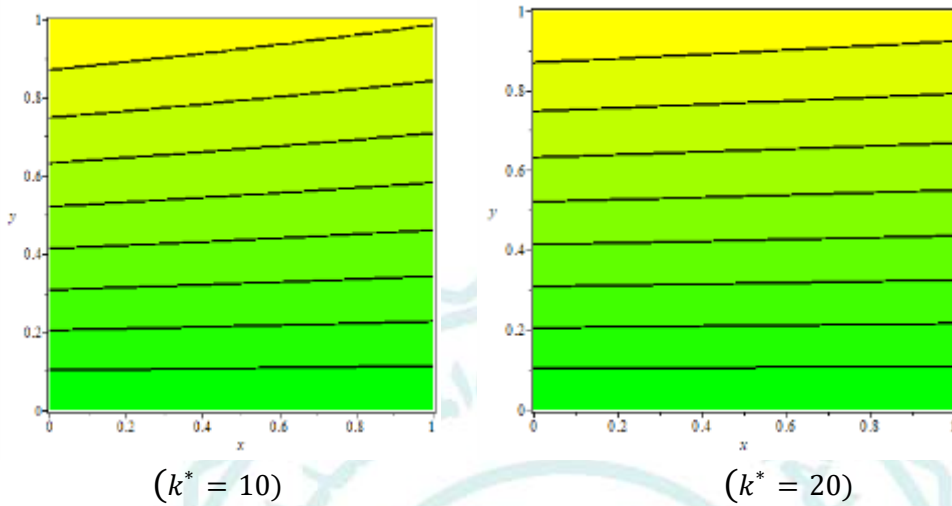


Figure.11. The counter of the vorticity function for  $R_E = 1.5$ ,  $M_G = 0.5$ ,  $\vartheta = 0$ , and  $M_P = 0.7$ .

## 8. Conclusion

A theoretical study of an unsteady a viscous MHD of squeezing flow fluid passing in porous medium among two infinite parallel plates is performed. The perturbation iteration technique is implemented to obtained approximate analytical solutions of proposed technique. The behavior of the velocity profile increases with the growth of the Reynolds number  $R_E$  while it can be seen decreasing with the rise of magnetic-hydrodynamic parameter  $M_G$  and porous parameter  $M_P$ . The results of PIT were compared with HPM, RKF5 and RK4 the results obtained using this technique confirm that it is more effective with a consistent approach in terms of low computational cost and accuracy compared to other methods. Furthermore, the results obtained using this technique confirm that it is fully compatible with the numerical solution obtained by the RKF5 method.

## REFERENCES

- [1] X. J. Ran, Q. Y. Zhu, and Y. Li, "An explicit series solution of the squeezing flow between two infinite plates by means of the homotopy analysis method," Communications in Nonlinear Science and Numerical Simulation, vol. 14, no. 1, pp. 119–132,2009.
- [2] N. A. M. Noor, S. Shafie, and M. A. Admon, Heat and mass transfer on MHD squeezing flow of Jeffrey nanofluid in horizontal channel through permeable medium," PLoS One, vol. 16, no. 5, Article ID e0250402, 2021.

- [3] Al-Saif, A. J. A., and Abeer Majeed Jasim. A new analytical-approximate solution for the viscoelastic squeezing flow between two parallel plates." Applied Mathematics and Information Sciences 13 (2019): 173-182. <https://doi.org/10.18576/amis/130204>.
- [4] Jasim A. Majeed, "Study of Impact of Unsteady Squeezing Magnetohydrodynamics Capper-Water with Injection-Suction on Nanofluid Fluid Between Two Parallel Plates in Porous Medium," Iraqi Journal of Science, vol. 63, no. 9, pp. 3909-3924, 2022.
- [5] M.J. Stefan, Versuch Uber die scheinbare adhesion, Sitzungsberichte der Akademie der Wissenschaften in Wien, Math. - Naturwissen 69 (1874) 713–721.
- [6] E. R. Maki, D. C. Kuzma, and R. J. Donnelly, Magnetohydrodynamic lubrication flow between parallel plates, Journal of Fluid Mechanics, vol. 26, no. 3, pp. 537–543, 1966.
- [7] Takhar, Harmindar S., Ali J. Chamkha, and Girishwar Nath. "MHD flow over a moving plate in a rotating fluid with magnetic field, Hall currents and free stream velocity." International Journal of Engineering Science. 40, no. 13 (2002): 1511-1527. [https://doi.org/10.1016/S0020-7225\(02\)00016-2](https://doi.org/10.1016/S0020-7225(02)00016-2).
- [8] Chamkha, Ali J. "Hydromagnetic two- phase flow in a channel." International journal of engineering science 33, no. 3 (1995): 437-446. [https://doi.org/10.1016/0020-7225\(93\)E0006-Q](https://doi.org/10.1016/0020-7225(93)E0006-Q).
- [9] Selimefendigil, Fatih, Hakan F. Oztop, and Ali J. Chamkha. "Role of magnetic field on forced convection of nanofluid in a branching channel." International Journal of Numerical Methods for Heat & Fluid Flow (2019). <https://doi.org/10.1108/HFF-10-2018-0568>.
- [10] Chamkha, Ali J. "Unsteady laminar hydromagnetic fluid–particle flow and heat transfer in channels and circular pipes." International Journal of Heat and Fluid Flow 21, no. 6 (2000): 740-746. [https://doi.org/10.1016/S0142-727X\(00\)00031-X](https://doi.org/10.1016/S0142-727X(00)00031-X).
- [11] K. S. Sorbie, "Depleted layer effects in polymer flow through porous media," Journal of Colloid and Interface Science, vol. 139, no. 2, pp. 299–314, 1990.
- [12] S. Luk, R. Mutharasan, and D. Apelian, "Experimental observations of wall slip: tube and packed bed flow," Industrial & Engineering Chemistry Research, vol. 26, no. 8, pp. 1609–1616, 1987.
- [13] C. Neto, D. R. Evans, E. Bonaccorso, H.-J. Butt, and V. S. J. Craig, "Boundary slip in Newtonian liquids: a review of experimental studies," Reports on Progress in Physics, vol. 68, no. 12, pp. 2859–2897, 2005.
- [14] M. Qayyum, H. Khan, and O. Khan, "Slip analysis at fluidsolid interface in MHD

squeezing flow of Casson fluid through porous medium,” Results in Physics, vol. 7, pp. 732–750, 2017.

[15] R. F. Westover, “The significance of slip of polymer melt flow,” Polymer Engineering & Science, vol. 6, no. 1, pp. 83–89, 1966

[16] M. Mooney, Explicit formulas for slip and fluidity, Journal of Rheology, vol. 2, no. 2, pp. 210–222, 1931.

[17] R. Buscall, “Letter to the editor: wall slip in dispersion rheometry,” Journal of Rheology, vol. 54, no. 6, pp. 1177–1183, 2010.

[18] A. M. Siddiqui, S. Irum, and A. R. Ansari, “Unsteady squeezing flow of a viscous MHD fluid between parallel plates, a solution using the homotopy perturbation method,” Mathematical Modelling and Analysis, vol. 13, no. 4, pp. 565–576, dec 2008.

[19] N. B. Dik, General Convergence Analysis for the Perturbation-Iteration Technique, Turk. J. Math. Comput. Sci. 6,2017, 1-9.

[20] J. Al-Saifi, J. Harfash, Perturbation-Iteration Algorithm for Solving Heat and Mass Transfer in the Unsteady Squeezing Flow between Parallel Plates,

[21] Jasim, Abeer Majeed, Exploration of No-Slip and Slip of Unsteady Squeezing Flow Fluid Through a Derivatives Series Algorithm, Journal of Advanced Research in Fluid Mechanics and Thermal Sciences, vol. 100, no. 1, pp. 11-29, 2022.

[22] Qayyum, Mubashir, and Imbsat Oscar. Exploration of Unsteady Squeezing Flow through Least Squares Homotopy Perturbation Method. Journal of Mathematics (2021). <https://doi.org/10.1155/2021/2977026>.